韓國水資源學會論文集
第31卷 第2號 · 1998年 4月
pp. 177~187

지하수 분산오염원에 대한 공간적분모형과 공간분포모형의 비교

Comparison between the Spatially Integrated Model and the Spatially Distributed Model in the Nonpoint Source Contaminants of Groundwater

이 도 훈* / 이 은 태* / 정 상 만** / 문 수 남***
Lee, Do-Hun / Lee, Eun-Tae / Jeong, Sang-Man / Moon, Soo-Nam

Abstract

The spatially integrated model (SIM) which can evaluate temporal variation of groundwater quality is proposed in the stream aquifer setting entered by nonpoint source contaminants. And the developed SIM included unsaturated soil zone and was tested against the spatially distributed model (SDM) of the coupled advection dispersion and Richards equations for the various hydrologic and aquifer simulating conditions. The result of the comparison showed that the average concentration responses of saturated aquifer and groundwater outflow between the SIM and the SDM was in good agreement, except for the cases of the large dispersivity ratio and thick aquifer system. And it is shown that for the cases of the large dispersivity ratio and thick aquifer system the performance of the nonlinear SIM is better than that of the linear SIM for evaluating the average concentration of groundwater outflow response.

Keywords : aquifer-stream interaction, groundwater quality modeling, nonpoint source pollution, unsaturated flow

요 지

하천과 대수층이 연결된 계에서 분산오염원이 유입될 경우에 지하수 수질을 평가할 수 있는 공간적분모형을 제안하였다. 제안된 공간적분모형은 불포화대의 영향이 고려되었으며, 다양한 수문 및 대수층 모의조건에서 Richards 방정식과 이송 분산 방정식의 공간분포모형에 대한 수치해와 비교를 통하여 공간적분모형을 테스트하였다. 비교결과에 의하면, 분산도비와 대수층의 두께가 큰 경우를 제외하고는 공간적분모형과 공간분포모형사이의 포화대수층의 평균농도 및 지하수유출의 평균농도는 일치된 반응을 보여주고 있다. 그리고 분산도비와 대수층의 두께가 큰 계에서는 비선형 공간적분모형이 선형 공간적분모형보다 더 좋은 결과를 보여주었다.

핵심용어 : 대수층-하천의 상호작용, 지하수수질 모델링, 분산오염원, 불포화흐름

* 경희대학교 공과대학 토목공학과 및 환경연구소 조교수
* 경희대학교 공과대학 토목공학과 교수
** 공주대학교 공과대학 토목공학과 조교수
*** 육군사관학교 토목공학과 강사

1. Introduction

In this paper, the spatially integrated model (SIM) considering the unsaturated soil zone is proposed and tested for the evaluation of nonpoint contaminants response in the groundwater-stream system. The motivation for developing this kind of spatially integrated models is due to a simple structure of the model such that the data requirements for the model are minimized compared with the distributed transport groundwater models. However, since the SIM neglects the spatial coordinates, only temporal responses for the averaged concentration of groundwater outflow and saturated aquifer can be determined. Hence, the spatially integrated model might be very useful for the long-term and/or preliminary assessment of groundwater outflow quality for nonpoint source pollution when the available data and resources are limited.

Perhaps, Gelhar and Wilson (1974) were the first researchers to propose the lumped parameter model based on water and mass balance equations, and complete mixing assumption. For the present context, the lumped parameter model is the same meaning as a linear reservoir model or the SIM. In the past, the lumped parameter model of Gelhar and Wilson (1974) has been applied for a number of studies for the evaluation of nonpoint source pollution in the saturated unconfined aquifer-stream setting (McLin, 1981; Duffy and Gelhar, 1985, 1986). And Duffy and Lee (1992) tested the linear reservoir model in the situation of heterogeneous and saturated unconfined aquifer-stream system.

Since the SIM for assessing groundwater outflow quality has not included the important effect of unsaturated soil zone, there is a need to develop and to test the SIM in order to account for the effect of unsaturated soil zone. In this paper, we proposed the linear SIM which accounted for unsaturated soil zone and tested the performance of the linear SIM through the comparison with the spatially distributed model (SDM). For the performance test between the SIM and the SDM, the responses of average concentration of saturated aquifer $\langle C_s \rangle$ and the average concentration of groundwater outflow $\langle C_q \rangle$ were compared under a variety of simulating conditions. The simulation factors considered in the model test were the variations in the dispersivity ratio, stream penetrating depth, aquifer thickness, rainfall rate, and soil type. Since the linear SIM have compared poorly with the SDM for the cases of large aquifer thickness and the large ratio of longitudinal dispersivity to the transverse dispersivity, the nonlinear SIM was introduced and compared with the SDM. It was shown that the response errors between the SIM and the SDM were reduced by applying the nonlinear SIM. The limiting elements for the model testing might be the effects of heterogeneous and anisotropic medium, transient flow, chemical reaction, and other sources/sinks.

2. Structure for Models

2.1 Spatially Integrated Model (SIM)

The SIM has the physical basis and can be developed by combining the integral mass balance equation with the well-mixing assumption for unsaturated and saturated flow zones. The integral mass balance equations for unsaturated and saturated flow zones are given by

$$\frac{d}{dt}(V_u(t) \cdot \langle C_u(t) \rangle) = I(t) \times \langle C_i(t) \rangle - R(t) \times \langle C_r(t) \rangle \quad (1a)$$

$$\frac{d}{dt}(V_s(t) \cdot \langle C_s(t) \rangle) = R(t) \times \langle C_r(t) \rangle - Q(t) \times \langle C_q(t) \rangle \quad (1b)$$

where $V_u(t)$ is the unsaturated soil moisture storage, $V_s(t)$ is the saturated aquifer water storage, $I(t)$ is the space integrated infiltration rate, $R(t)$ is the space integrated recharge rate, and $Q(t)$ is the space integrated groundwater outflow. The space averaged input concentration is indicated by $\langle C_i(t)\rangle$. The spatial average concentration of unsaturated soil zone $\langle C_u(t)\rangle$ is defined by

$$\langle C_u(t)\rangle = \frac{\int\int\int_{uz}\theta(\boldsymbol{x}, t)C(\boldsymbol{x}, t)dzdydx}{\int\int\int_{uz}\theta(\boldsymbol{x}, t)dzdydx}$$

where $\theta(\boldsymbol{x}, t)$ is the soil moisture content, and uz represents the domain of unsaturated soil zone. The spatial average concentration of recharge $\langle C_r(t)\rangle$ is defined by

$$\langle C_r(t)\rangle = \frac{\int\int_{rb}(\boldsymbol{v}(\boldsymbol{x}_r, t)\cdot\boldsymbol{n}_r)C(\boldsymbol{x}_r, t)dB}{\int\int_{rb}(\boldsymbol{v}(\boldsymbol{x}_r, t)\cdot\boldsymbol{n}_r)dB}$$

where rb is the domain of recharge boundary surface. The Darcy velocity vector along the recharge boundary rb is represented by $\boldsymbol{v}(\boldsymbol{x}_r, t)$ and the unit vector normal to the recharge boundary by $\boldsymbol{n}_r$. Thus, the term $(\boldsymbol{v}(\boldsymbol{x}_r, t)\cdot\boldsymbol{n}_r)$ means the recharge water flux into the water table. The spatial average concentration of saturated aquifer $\langle C_s(t)\rangle$ is defined by

$$\langle C_s(t)\rangle = \frac{\int\int\int_{sz}\theta_s(\boldsymbol{x}, t)C(\boldsymbol{x}, t)dzdydx}{\int\int\int_{sz}\theta_s(\boldsymbol{x}, t)dzdydx}$$

where sz represents the domain of saturated aquifer and $\theta_s(\boldsymbol{x}, t)$ is the saturation moisture content. The spatial average concentration of groundwater outflow $\langle C_q(t)\rangle$ is defined by

$$\langle C_q(t)\rangle = \frac{\int\int_{ob}(\boldsymbol{v}(\boldsymbol{x}_q, t)\cdot\boldsymbol{n}_q)C(\boldsymbol{x}_q, t)dB}{\int\int_{ob}(\boldsymbol{v}(\boldsymbol{x}_q, t)\cdot\boldsymbol{n}_q)dB}$$

where ob represents the domain of boundary surface for groundwater outflow. The Darcy velocity vector along the outflow boundary ob is represented by $\boldsymbol{v}(\boldsymbol{x}_q, t)$ and the unit vector normal to the outflow boundary by $\boldsymbol{n}_q$. The term $(\boldsymbol{v}(\boldsymbol{x}_q, t)\cdot\boldsymbol{n}_q)$ indicates the groundwater outflow flux from saturated aquifer.

When the flow field is assumed to be steady state, the following conditions are satisfied: $\frac{dV_u(t)}{dt} = 0 = I(t) - R(t)$ and $\frac{dV_s(t)}{dt} = 0 = R(t) - Q(t)$ Hence, the Eqns. 1(a) and 1(b) can be transformed as follows.

$$\frac{d\langle C_u(t)\rangle}{dt} = \frac{I(t)}{V_u(t)}\langle C_i(t)\rangle - \frac{R(t)}{V_u(t)}\langle C_r(t)\rangle \quad (2a)$$

$$\frac{d\langle C_s(t)\rangle}{dt} = \frac{R(t)}{V_s(t)}\langle C_r(t)\rangle - \frac{Q(t)}{V_s(t)}\langle C_q(t)\rangle \quad (2b)$$

If we assume the well-mixing assumption of $C_r(t) = C_u(t)$ and $C_q(t) = C_s(t)$ and use the definition for $T_u = V_u/R$and $T_s = V_s/Q$ then we obtain the SIM 3(a)~3(d) from Eqns. 2(a) and 2(b).

$$\frac{d\langle C_u(t)\rangle}{dt} = \frac{\langle C_i(t)\rangle}{T_u} - \frac{\langle C_u(t)\rangle}{T_u} \quad (3a)$$

$$\frac{d\langle C_r(t)\rangle}{dt} = \frac{d\langle C_u(t)\rangle}{dt} \quad (3b)$$

$$\frac{d\langle C_s(t)\rangle}{dt} = \frac{\langle C_r(t)\rangle}{T_s} - \frac{\langle C_s(t)\rangle}{T_s} \quad (3c)$$

$$\frac{d\langle C_q(t)\rangle}{dt} = \frac{d\langle C_s(t)\rangle}{dt} \quad (3d)$$

In the Eqns. 3(a)~3(d), the dynamical behaviour for $C_r(t)$ is completely determined by $C_u(t)$ and $C_q(t)$ variable is also completely determined by $C_s(t)$ such that the system is governed by two state variables $C_u(t)$ and $C_s(t)$. Two parameters involved in the SIM are average solute residence time of unsaturated zone (T_u) and average solute residence time of saturated zone (T_s). And these paramaters are conveniently estimated by $T_u = V_u / R$ and $T_s = V_s / Q$

2.1.1 Dimensionless system

The SIM 3(a)~3(d) can be transformed into a dimensionless SIM for the generalization of solution results such that the following dimensionless variables can be defined

$$t^* = \frac{t}{T_s},\ \langle C_u^*(t^*) \rangle = \frac{\langle C_u(t) \rangle}{C_o},$$

$$\langle C_r^*(t^*) \rangle = \frac{\langle C_r(t) \rangle}{C_o},\ \langle C_s^*(t^*) \rangle = \frac{\langle C_s(t) \rangle}{C_o}$$

$$\langle C_q^*(t^*) \rangle = \frac{\langle C_q(t) \rangle}{C_o},\ \langle C_i^*(t^*) \rangle = \frac{\langle C_i(t) \rangle}{C_o}$$

where C_o is a characteristic concentration. By substituting these dimensionless variables into the Eqns. 3(a)~3(d), we obtain the dimensionless form of SIM as follows.

$$\frac{d\langle C_u^*(t^*) \rangle}{dt^*} = \frac{T_s}{T_u}(\langle C_i^*(t^*) \rangle - \langle C_u^*(t^*) \rangle) \quad (4a)$$

$$\frac{d\langle C_r^*(t^*) \rangle}{dt^*} = \frac{d\langle C_u^*(t^*) \rangle}{dt^*} \quad (4b)$$

$$\frac{d\langle C_s^*(t^*) \rangle}{dt^*} = \langle C_r^*(t^*) \rangle - \langle C_s^*(t^*) \rangle \quad (4c)$$

$$\frac{d\langle C_q^*(t^*) \rangle}{dt^*} = \frac{d\langle C_s^*(t^*) \rangle}{dt^*} \quad (4d)$$

A system of ordinary differential Eqns. 4(a)~4(d) is linear and can be solved with the given initial conditions ($\langle C_u^*(0) \rangle$ and $\langle C_s^*(0) \rangle$), input concentration $\langle C_i^*(t^*) \rangle$ and parameter values of T_u and T_s.

2.2 Spatially Distributed Model (SDM)

For the present context the spatially distributed model is meant to be an advection-dispersion equation which requires spatially distributed parameters and conditions. In the soil and aquifer system, the advection-dispersion equation without the effects of sources/sinks, and reactions might be described by coupling Fick's law and the mass conservation principle (Bear, 1972; Bear, 1979) as follows.

$$\theta \frac{\partial C}{\partial t} + \boldsymbol{v} \cdot \nabla C = \nabla \cdot (\theta \boldsymbol{D} \cdot \nabla C) \quad (5)$$

In Eqn. (5) θ is soil moisture content; C[M/L^3] is a concentration of dissolved solutes; $\boldsymbol{v}$[M/T] is Darcy velocity; $\boldsymbol{D}$[L^2/T] represents the hydrodynamic dispersion tensor given by

$$\theta \boldsymbol{D} = \alpha_T |\boldsymbol{v}| \boldsymbol{\delta} + (\alpha_L - \alpha_T) \boldsymbol{v}\boldsymbol{v} / |\boldsymbol{v}| + \theta a_m \boldsymbol{\tau} \quad (6)$$

where $|\boldsymbol{v}|$ is the absolute magnitude of $\boldsymbol{v}$, α_L is the longitudinal dispersivity, α_T is the transverse dispersivity, a_m is the molecular diffusion coefficient, $\boldsymbol{\delta}$ is Kronecker delta tensor, and $\boldsymbol{\tau}$ indicates the tortuosity that is the second rank symmetric tensor (Bear, 1979). It is implicitly assumed in the following numerical analyses that the molecular diffusion is negligible.

For unsaturated-saturated flow, Darcian velocity vector in Eqn. (5) takes the following form

$$\boldsymbol{v} = -K(h) \nabla h \quad (7)$$

where $K(h)$ is an unsaturated hydraulic conductivity that is dependent on the matric potential h or soil moisture θ. The matric potential or pressure head field in the Eqn. (7) can be determined by solving Richards equation (1931) that describes the unsaturated flow process. For steady-state flow, Richards equation is given by combining Darcy flux of unsaturated flow with the continuity equation as follows.

$$\nabla \cdot [K(h) \nabla h + \nabla Z] = 0 \quad (8)$$

In order to solve the Eqn. (8), the characteristic curves for the h and $K(h) - h$ relations need to be specified. In this study we used soil hydraulic properties reported in Carsel and Parrish (1988).

3. Comparison of Responses between Models

In order to evaluate the validity of the proposed SIM, a solution to the SIM 4(a)~4(d) is compared with that of the SDM (5) and (8) for the various transport controlling factors and conditions as shown in Table 1. Fig. 1 illustrates the geometry of the system in the two dimensional cross section. This groundwater-stream connected geometry is the same as that studied in Lee et al.

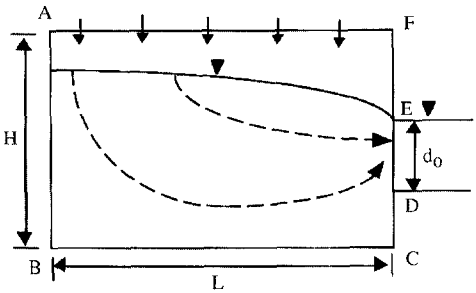

Fig. 1. Two Dimensional Groundwater -Stream System(L=Aquifer Length, H=Aquifer Thickness, d_0=Stream Depth)

(1998) which investigated the effects of transport controlling factors on the integral concentration of groundwater based on the coupled advection-dispersion and Richards equations. For all cases examined in the analyses, the initial concentration values were specified as zero and the input concentration at the ground surface is maintained a constant throughout the simulation time. Numerical simulation aspects for solving the SDM can be found in the references (Yeh, 1987; Yeh et al., 1992; Yeh and Chang, 1993; Lee et al., 1998).

3.1 Cases of Dispersivity Changes

Fig. 2 shows the comparison of $\langle C_s^* \rangle$ and $\langle C_q^* \rangle$ responses between SIM and SDM for three different dispersivity ratios as summarized in Table 1. The root mean square error (rmse) was used for a measure of error between two models and defined by

$$\text{rmse} = \sqrt{\frac{\sum(\langle C_k^*(t^*)\rangle_I - \langle C_k^*(t^*)\rangle_D)^2}{n}}$$

where $\langle C_k^*(t^*)\rangle_I$ is $\langle C_s^* \rangle$ or $\langle C_q^* \rangle$ responses resulted from SIM, and $\langle C_k^*(t^*)\rangle_D$ is $\langle C_s^* \rangle$ or $\langle C_q^* \rangle$ responses resulted from

Table 1. The Simulating Parameter Values and Conditions

case	$\alpha_L(m)$	α_L/α_T	d_0/H	H/L	Rainfall rate (m/hr)	soil type	T_u (years)	T_s (years)
1	1	10	0.25	0.1	3.12*10 [illegible]	Loam soil	1.36	13.84
2	0.1	1	"	"	"	"	"	"
3	50	500	"	"	"	"	"	"
4	1	10	0.1	"	"	"	1.32	13.94
5	"	"	0.7	"	"	"	1.41	13.74
6	"	"	0.25	0.3	"	"	1.99	44.3
7	"	"	"	0.5	"	"	1.96	75.75
8	"	"	"	0.1	5.2*10 [illegible]	"	13.04	73.16
9	"	"	"	"	1.04*10 [illegible]	"	5.95	37.82
10	"	"	"	"	"	Sandy Loam soil	3.81	34.88
11	"	"	"	"	"	Silt Loam soil	6.15	41.84

(α_L=longitudinal dispersivity, α_T=transverse dispersivity, L=aquifer length, H=aquifer thickness, d_o=stream depth, T_u=average residence time of unsaturated zone, T_s=average residence time of saturated zone)

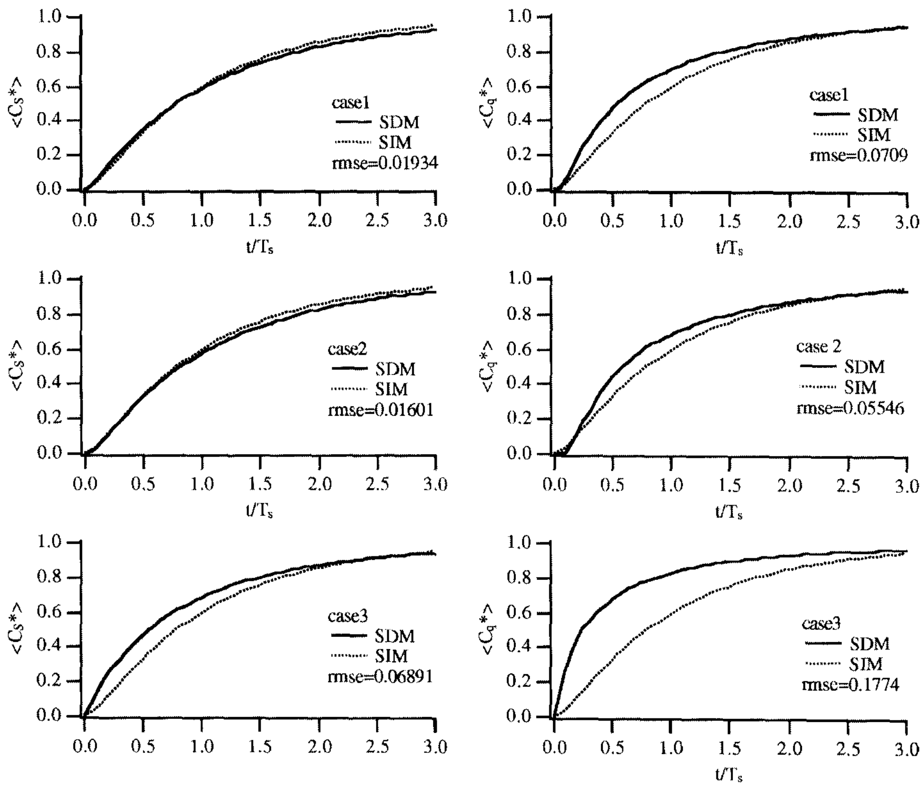

Fig. 2. Comparison of Responses for the Different Dispersivity Ratios

SDM; n is the number of data.

In Fig 2 the $\langle C_s^* \rangle$ responses between SIM and SDM are in close agreement, but the rmse increases as the dispersivity ratio(α_L / α_T) increases. The $\langle C_q^* \rangle$ response of the SIM underestimated that of the SDM and the rmse grows when the dispersivity ratio increases. The substantial difference for $\langle C_q^* \rangle$ response between models exist for case 3 with the dispersivity ratio of 500. Hence, these results suggest that the linear SIM 4(a)~4(d) is unable to describe exactly the dynamic behaviour of $\langle C_q^* \rangle$ variable for various ranges of dispersivity ratios. The physical reason for poor performance of the SIM is that the degree of nonlinearity for $\langle C_s^* \rangle - \langle C_q^* \rangle$ relationship increases as the dispersivity ratio increase, which was suggested by numerical simulation results of Lee et. al. (1998). Later, we will propose the nonlinear SIM to improve the performance of the linear SIM.

3.2 Cases of Stream Depth Changes

In order to understand the effect of the stream depth variations on the performance of the SIM, the comparison of model responses is performed for the different stream penetrating depths that is specified as the part of the boundary conditions for the SDM. Fig. 3 shows the comparison of $\langle C_s^* \rangle$ and $\langle C_q^* \rangle$ responses between SIM and SDM. The $\langle C_s^* \rangle$ response is in good agreement between two models and the rmse for $\langle C_s^* \rangle$ response is smaller than that of $\langle C_q^* \rangle$ response. For case 1 and case 4 of partially penetrating stream depth, the $\langle C_q^* \rangle$ response for SIM is slightly smaller than the $\langle C_q^* \rangle$ response

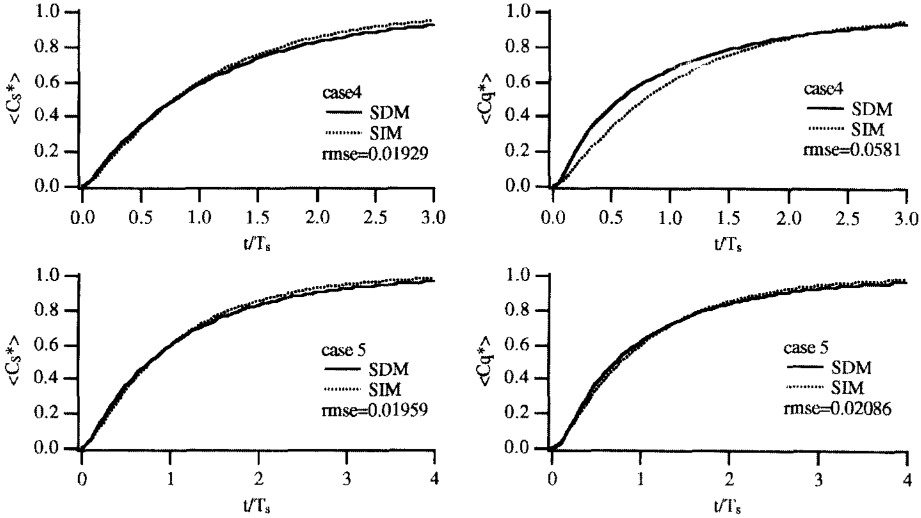

Fig. 3. Comparison of Responses for the Different Stream Depths

for SDM, but the $\langle C_q^* \rangle$ response between two models in case 5 of the fully penetrating stream depth shows an identical $\langle C_q^* \rangle$ response. The physical explanation is that the groundwater outflow boundary enlarges for the fully penetrating stream depth such that the enhanced mixing process at the stream boundary makes the $\langle C_s^* \rangle$-$\langle C_q^* \rangle$ relationship linear. This physical mechanism is also revealed by the $\langle C_s^* \rangle - \langle C_q^* \rangle$ relationship from numerical simulation results of Lee et al. (1998).

3.3 Cases of Aquifer Thickness Changes

Fig. 4 shows the comparison of $\langle C_s^* \rangle$ and

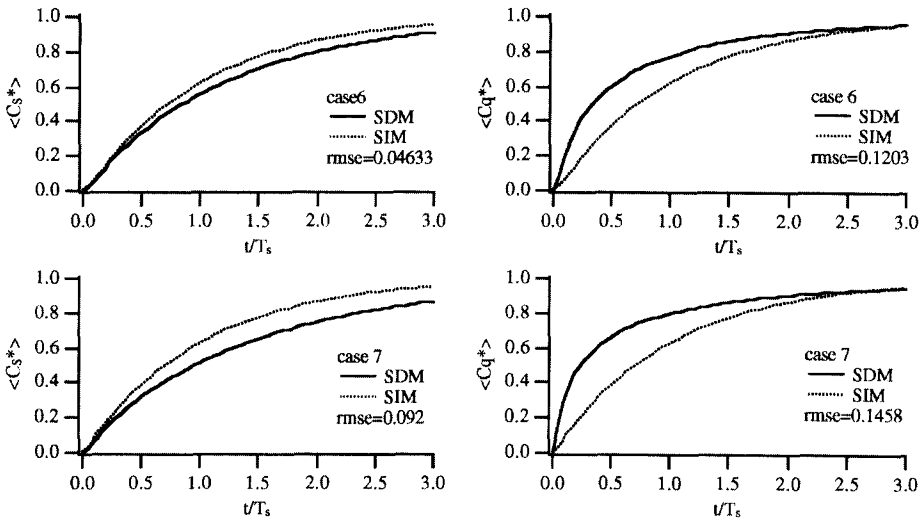

Fig. 4. Comparison of Responses for the Different Aquifer Thickness

$\langle C_q^* \rangle$ responses between SIM and SDM subject to the changes in aquifer thickness or aquifer aspect ratio H/L. The rmse errors of case 6 with H/L=0.3 for both $\langle C_s^* \rangle$ and $\langle C_q^* \rangle$ responses are shown to be smaller than that of case 7 of H/L=0.5. The $\langle C_s^* \rangle$ responses of the SIM slightly overestimated the $\langle C_s^* \rangle$ responses of the SDM for both cases. However, the $\langle C_q^* \rangle$ response exhibit a reverse pattern compared to the $\langle C_s^* \rangle$ response such that the response of SIM underestimated the response of SDM. And there is a significant difference of $\langle C_q^* \rangle$ response between the SIM and the SDM. As for a large dispersivity ratio, the poor performance of the SIM lies in the fact that the linear relationship between $\langle C_s^* \rangle$ and $\langle C_q^* \rangle$ assumed in the SIM does not hold for the large aspect ratio.

3.4 Cases of Rainfall Rate Changes

The effect of the rainfall rate variations on the performance of the SIM was investigated as shown in Fig. 5. The $\langle C_s^* \rangle$ response between the SIM and the SDM is in good argeement with a relatively small rmse. The $\langle C_q^* \rangle$ response of the SIM is seen to be underestimated compared to the $\langle C_q^* \rangle$ response of the SDM. And the rmse errors of $\langle C_s^* \rangle$ and $\langle C_q^* \rangle$ responses between case 8 and case 9 are shown to be very close to each other. So it implies that the performance of the SIM is compared with that of the SDM for different steady rainfall rates.

3.5 Cases of Soil type changes

Sandy loam and silt loam soil were used to test the impact of soil types on the performance of the SIM. The hydraulic conductivity of sandy loam soil is about 10 times as that of silt loam and characteristic curves for soil moisture-pressure head and unsaturated hydraulic conductivity -pressure head are very different between two soils (Carsel and Parrish, 1988). Fig. 6 shows the comparison of $\langle C_s^* \rangle$ and $\langle C_q^* \rangle$ responses between the SIM and the SDM. In case 10 of sandy loam soil the $\langle C_s^* \rangle$ response of the SIM is almost identical to that of the SDM, showing smaller rmse value than case 11 of silt loam soil. In case 11, the $\langle C_s^* \rangle$ response of the SIM overestimated that of the SDM. For the $\langle C_q^* \rangle$ responses, the rmse of silt loam is slightly smaller than that of sandy loam. Overall, the SIM describes reasonably the response of the SDM for different soil types.

4. Concluding Remarks and Discussion

The spatially integrated model is proposed to assess the average concentration of saturated aquifer $\langle C_s^* \rangle$ and the average concentration of groundwater outflow $\langle C_q^* \rangle$ from nonpoint source contaminants in stream connected groundwater system. Compared to previous studies, this study included an unsaturated soil zone in the model development and testing. The performance test shows that the SIM responses are fairly compared with the SDM responses.

In general, the rmse errors for $\langle C_q^* \rangle$ variable are larger than the rmse errors of $\langle C_s^* \rangle$ variable. And for a large dispersivity ratio and a thick aquifer condition, the SIM describes poorly the dynamic behaviour of $\langle C_q^* \rangle$ variable of the SDM, showing a relatively large rmse error. This poor prediction of the SIM is in contrast to the result of Duffy and Lee (1992) who investigated the comparison of the SIM to the SDM only in the saturated aquifer condition. They showed that the dynamic $\langle C_q^* \rangle$ behaviour between the SIM and the SDM was in good agreement under various dispersivity ratios and aquifer aspect ratios of less than 4. The linear SIM 4(a)~4(d) does not account for the increased degree of the nonlinear

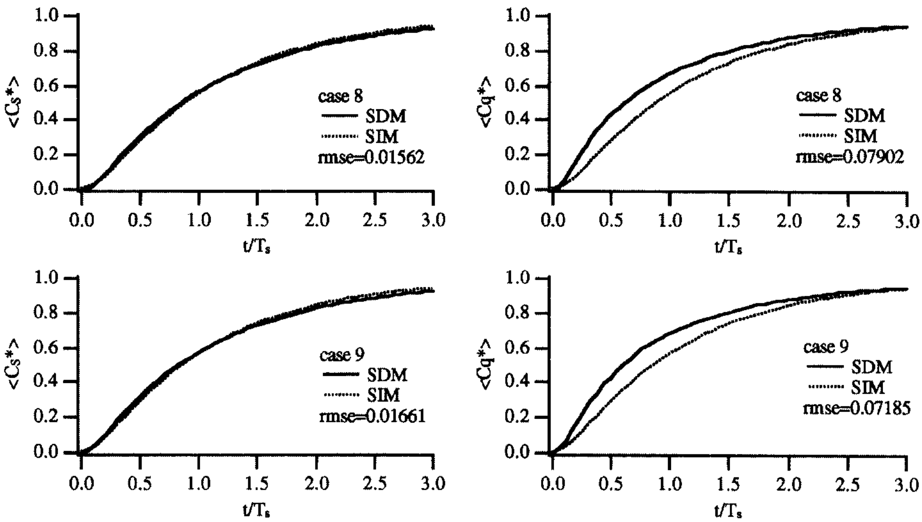

Fig. 5. Comparison of Responses for the Different Rainfall Rates

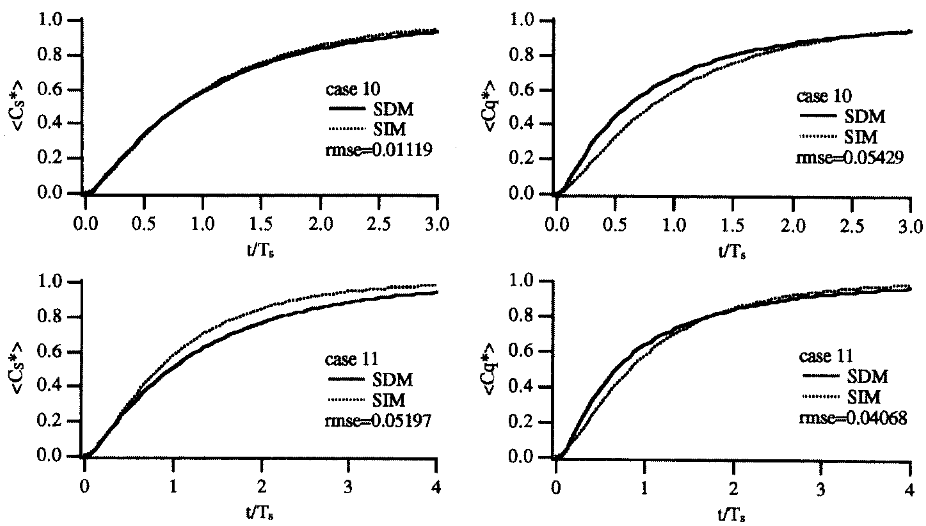

Fig. 6. Comparison of Responses for the Different Soil Types.

relationship between $\langle C_s^* \rangle$ and $\langle C_q^* \rangle$ as the dispersivity ratio and aquifer aspect ratio increase. So there is a need to improve the predictive ability of the SIM for the various ranges of the dispersivity ratio and aquifer aspect ratio parameters. Instead of assuming $\frac{d\langle C_q^*(t^*)\rangle}{dt^*} = \frac{d\langle C_s^*(t^*)\rangle}{dt^*}$ in the SIM 4(a)~4(d), we can use the nonlinear functional relationship between $\langle C_s^* \rangle$ and $\langle C_q^* \rangle$ defined as

Table 2. Coefficients of Nonlinear Fitting Model
$\langle C_q^* \rangle = a_1 \langle C_s^* \rangle + a_2 \langle C_s^* \rangle^2 + a_3 \langle C_s^* \rangle^3 + a_4 \langle C_s^* \rangle^4 + a_5 \langle C_s^* \rangle^5$ for Three Cases

case	a_1	a_2	a_3	a_4	a_5
3	2.28985	-2.16116	0.872929	0	0
6	3.75939	-10.3155	18.1163	-16.0476	5.49555
7	5.12257	16.6901	30.3236	-26.8797	9.1376

$$\langle C_q^* \rangle = a_1 \langle C_s^* \rangle + a_2 \langle C_s^* \rangle^2 + a_3 \langle C_s^* \rangle^3 + a_4 \langle C_s^* \rangle^4 + a_5 \langle C_s^* \rangle^5$$

As shown in Table 2, the coefficients a_1, a_2, a_3, a_4, a_5 were determined by the fitting procedure using $\langle C_s^* \rangle$ and $\langle C_q^* \rangle$ data obtained from the numerical analysis of the SDM. And then the differentiation of the functional relation with respect to time provides the nonlinear SIM as follows.

$$\frac{d\langle C_u^*(t^*) \rangle}{dt^*} = \frac{T_s}{T_u}(\langle C_i^*(t^*) \rangle - \langle C_u^*(t^*) \rangle) \quad (9a)$$

$$\frac{d\langle C_r^*(t^*) \rangle}{dt^*} = \frac{d\langle C_u^*(t^*) \rangle}{dt^*} \quad (9b)$$

$$\frac{d\langle C_s^*(t^*) \rangle}{dt^*} = \langle C_r^*(t^*) \rangle - \langle C_s^*(t^*) \rangle \quad (9c)$$

$$\frac{d\langle C_q^*(t^*) \rangle}{dt^*} = [a_1 + 2a_2 \langle C_s^*(t^*) \rangle + 3a_3 \langle C_s^*(t^*) \rangle^2 + 4a_4 \langle C_s^*(t^*) \rangle^3 + 5a_5 \langle C_s^*(t^*) \rangle^4] \frac{d\langle C_s^*(t^*) \rangle}{dt^*} \quad (9d)$$

Fig. 7 shows the performance of the nonlinear SIM 9(a)~9(d) for case 3 of α_L/α_T=500, case 6 of H/L=0.3, and case 7 of H/L=0.5. We can recognize the reduced rmse errors for $\langle C_q^* \rangle$ variable by comparing Fig. 7 with Fig. 2 and Fig. 4.

In this research the effects of heterogeneous and anisotropic medium properties, and complex input concentration conditions have not yet examined such that further testing and development of the SIM are needed. And in order to apply the SIM for the assessment of nonpoint source groundwater

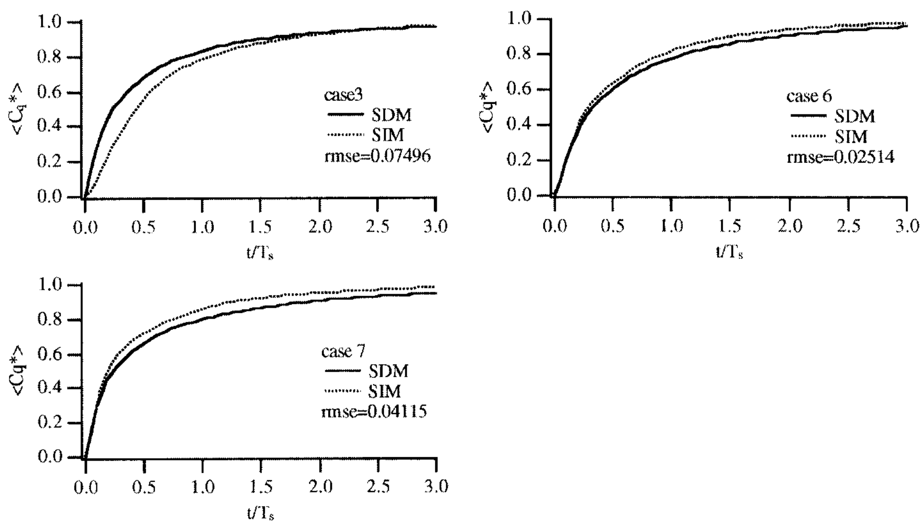

Fig. 7. Comparison of Responses between the Nonlinear SIM and SDM

problem there is a need for parameterizing the coefficients of the SIM in terms of measurable physical variables.

Acknowledgment

This research was supported by 1996 research grant from Kyung Hee University. This support is gratefully acknowledged.

References

Bear, J. (1972). *Dynamics of fluids in porous media*. Elsevier, New York, pp. 579-622.

Bear, J. (1979). *Hydraulics of Groundwater*. McGraw-Hill Inc, New York, pp. 225-243.

Carsel, R.F., and Parrish, R.S. (1988). "Developing joint probability distributions of soil water retention characteristics." *Water Resources Research*, Vol. 24, No. 5, pp. 755-769.

Duffy, C.J., and Gelhar, L.W. (1985). "A frequency domain approach to water quality modeling in groundwater: Theory." *Water Resources Research*, Vol. 21, No. 8, pp. 1175-1184.

Duffy, C.J., and Gelhar, L.W. (1986). "A frequency domain analysis of groundwater quality fluctuations : Interpretation of field data." *Water Resources Research*, Vol. 22, No. 7, pp. 1115-1128.

Duffy, C.J., and Lee, D.H. (1992). "Base flow response from nonpoint source contamination: Simulated spatial variability in source, structure, and initial condition." *Water Resources Research*, Vol. 28, No. 3, pp. 905-914.

Gelhar, L.W., and Wilson, J.L. (1997) "Ground-Water quality modeling." *Ground Water*, Vol. 12, No. 6, pp. 399-408.

Lee, D.H., Lee, E.T., and Lee, J.H. (1998). "Determining the Relationship between Average Concentration of Saturated Aquifer and Groundwater Outflow subject to Nonpoint Source Contaminants." Appear *in KSCE Journal of Civil Engineers*.

McLin, S.G. (1981). *Validity of the generalized lumped parameter hydrosalinity model in predicting irrigation return flow*. Ph.D. dissertation. New Mexico Institute of Mining and Technology, Socorro, New Mexico. pp. 1-475.

Richards, L.A. (1931). "Capillary conduction of liquids through porous medium." *Physics*, Vol. 1, pp. 318-333.

Yeh, G.T. (1987). FEMWTER: *A finite element model of water flow through saturated-unsaturated porous media - first revision*. ORNL-5567/RI. Oak Ridge National Laboratory. Oak Ridge, Tennessee, pp. 1-248.

Yeh, G.T., Sharp-Hansen, S., Lester B., Strobl, R., and Scarbrough, J. (1992). *3DFEMWATER /3DLEWASTE: Numerical codes for delineating wellhead protection areas in agricultural regions based on the assimilative capacity criterion*. EPA/600/R-92/223. Environmental Research Laboratory, U.S. Environmental Protection Agency. Athens, GA 30613.

Yeh, G.T., and Chang, J.R. (1993). *User's manual of a hybrid Lagrangian-Eulerian finite element model of waste transport through saturated-unsaturated media: Version 2.0*. Department of Civil Engineering, The Pennsylvania State University. PA. 16802.

<최종본 접수일 : 1998년 2월 5일>